Journal of Structural Geology 33 (2011) 662–675

Contents lists available at ScienceDirect

Journal of Structural Geology

journal homepage: www.elsevier.com/locate/jsg

# Relative strength of mafic and felsic rocks during amphibolite facies metamorphism and deformation

Mark A. Pearce [a,*], John Wheeler [b], David J. Prior [b]

[a] Geospatial Research Ltd., Department of Earth Science, University of Durham, Durham DH1 3LE, UK
[b] Department of Earth and Ocean Sciences, University of Liverpool, Liverpool L69 3GP, UK

ARTICLE INFO

*Article history:*
Received 18 March 2010
Received in revised form
4 January 2011
Accepted 8 January 2011
Available online 15 January 2011

*Keywords:*
Plagioclase
Amphibole
Deformation
EBSD

ABSTRACT

Field observations of mafic dykes intruded into felsic rocks from the Lewisian Complex, NW Scotland, suggest that the mafic rocks are weaker than the felsic ones, contrary to experimental results. In order to resolve this conflict, samples were studied to constrain the deformation mechanisms active under amphibolite facies conditions. Crystallographic preferred orientation (CPO) in plagioclase is used to infer deformation by dislocation creep on the $(112)[1\bar{1}0]$, $(1\bar{1}2)[110]$, $(001)[1\bar{1}0]$, and $(001)[\bar{1}\bar{1}0]$ slip systems. With increasing strain, this CPO became weaker due to grain-boundary sliding that accompanied diffusion creep. In rocks where grain size reduction of plagioclase occurred by chemically-dominated recrystallisation there is no CPO suggesting deformation was wholly accommodated by diffusion creep and grain-boundary sliding. In metamorphosed dykes, plagioclase grains have orientations that are not consistent with dislocation creep deformation. Amphibole has a CPO consistent with either dislocation creep on $\{100\}\langle001\rangle$ or deformation by diffusion creep with anisotropic dissolution and precipitation rates. It is inferred that metamorphism of the dykes lead to the production of fine-grained amphibole and plagioclase, both of which deform by diffusion creep, but that anisotropic dissolution and precipitation in the amphibole produced a CPO. The mafic dykes are weaker than the felsic gneisses because grain size reduction is more extreme in the dykes even though both may be deforming primarily by grain size sensitive mechanisms. This work highlights the variation in processes active in polyphase rocks and how these can lead to variations in CPO of the same mineral among different rock types.



## 1. Introduction

Exhumed high-grade terranes are essential to understanding lower crustal processes. Deformation of key minerals such as plagioclase (e.g. Rybacki and Dresen, 2004), amphibole (Tatham et al., 2008), and quartz (Hirth and Tullis, 1992) controls the strength of rock over a wide range of bulk compositions. Varying modal proportions (e.g. Rybacki and Dresen, 2000) and grain sizes (Rutter and Brodie, 1988) control which deformation mechanisms are active in which minerals and therefore the relative strength of the rocks (Handy, 1990). Whilst mafic rocks are usually considered stronger than felsic ones (e.g. Wilks and Carter, 1990), activity of grain size sensitive mechanisms and the production of weak phases (strain weakening e.g. Imon et al., 2002) may result in a reversal of this rheological contrast.

The Lewisian complex, NW Scotland, consists of mafic and felsic rocks that were variably deformed and metamorphosed to granulite and amphibolite facies a number of times during the Archaean and Palaeoproterozoic (Park and Tarney, 1987). Tonalite–trondhjemite–granodiorite gneisses were intruded by mafic (Scourie) dykes, which were themselves metamorphosed to amphibolite facies. Therefore, these rocks provide an opportunity to study the effects of microstructure and bulk rock composition on mineral deformation mechanism whilst minimising variations in other variables such as temperature.

In this paper, we employ electron backscatter diffraction (EBSD) to measure the crystallographic orientations of minerals in deformed amphibolite facies gneisses and dykes as part of the first detailed microstructural study of the quartzo-feldspathic gneisses from the Lewisian Complex. Outcrop scale field maps constrain the age of the deformation relative to dyke intrusion. Plagioclase fabrics are presented for rocks of different strains from a single outcrop and for different ages of deformation from a single sample. Plagioclase and amphibole fabrics are presented from deformed Scourie dykes. The difference in fabric strength is interpreted to result from different deformation mechanisms being active in different minerals. These interpretations are discussed in terms of

* Corresponding author. Fax: +44 0191 3343975.
*E-mail address:* mark@geospatial-research.co.uk (M.A. Pearce).

0191-8141/$ – see front matter © 2011 Elsevier Ltd. All rights reserved.
doi:10.1016/j.jsg.2011.01.002

the effects of strain on grain size and the relative strength of the different rocks within the Lewisian Complex, and lower crustal rocks in general.

## 2. Geologic setting

The Lewisian Gneiss Complex is exposed in the foreland of the Scottish Caledonides (Fig. 1a – inset). It is broadly divided into three regions with a central granulite region flanked by more intensely deformed amphibolite facies regions to the north and south. The complex is dominated by felsic to intermediate metaplutonic rocks (tonalite–trondhjemite–granodiorite, TTG) but also includes more mafic to ultramafic, metasedimentary, and metaigneous components. A suite of dykes of varying composition (from mafic to ultramafic) intrude the gneisses of the complex. Separating the northern and central regions is the high strain Laxford front. North of this tectonic zone the gneisses exhibit a folded shape fabric with a horizontal enveloping surface (Coward, 1984). The southern boundary of the central region is more complex involving a number of shear zones around Gairloch which cut and fold the metasediments and metaigneous rocks of the Loch Maree Group. The southernmost of the high strain zones is a km-scale zone exposed on the north and south shores of Loch Torridon (Fig. 1a), the Torridon high strain zone. Following a short description of the terminology used in this study, the geometry of the high strain zone and relationship between Scourie dykes and gneissic fabrics are documented. Finally, two study areas within the high strain zone and samples collected from these areas are outlined along with field constraints on their deformation kinematics and relative ages.

### 2.1. Nomenclature

Events prior to and following the Scourie dyke intrusion were termed Scourian and Laxfordian respectively (Sutton and Watson, 1950). With the recognition of a pre-dyke amphibolite facies event (Evans, 1965) the Scourian was subdivided into Badcallian (granulite facies, NE–SW trending fabrics) and Inverian (amphibolite facies, NW–SE trending fabrics) events. Fabrics were identified using these criteria and correlated across the complex. However, a model based primarily on dating of zoned zircon suggests that the complex comprises a number of disparate terranes assembled throughout the latest Archaean and Proterozoic (Kinny et al., 2005). Therefore, correlation of metamorphic and deformation episodes across terrane boundaries is not necessarily valid. However, since the age of deformation does not alter the kinematics or dynamics of the event then it is not important whether post-dyke deformation occurred at the same time everywhere or not. In the absence of other well defined nomenclature the term Badcallian will be used to refer to N–S to NE–SW location fabrics, and the terms, Inverian and Laxfordian to pre- and post-dyke events which produce NW–SE striking shape fabrics respectively. Similar features may not be the same age everywhere in the Lewisian (Kinny and Friend, 1997).

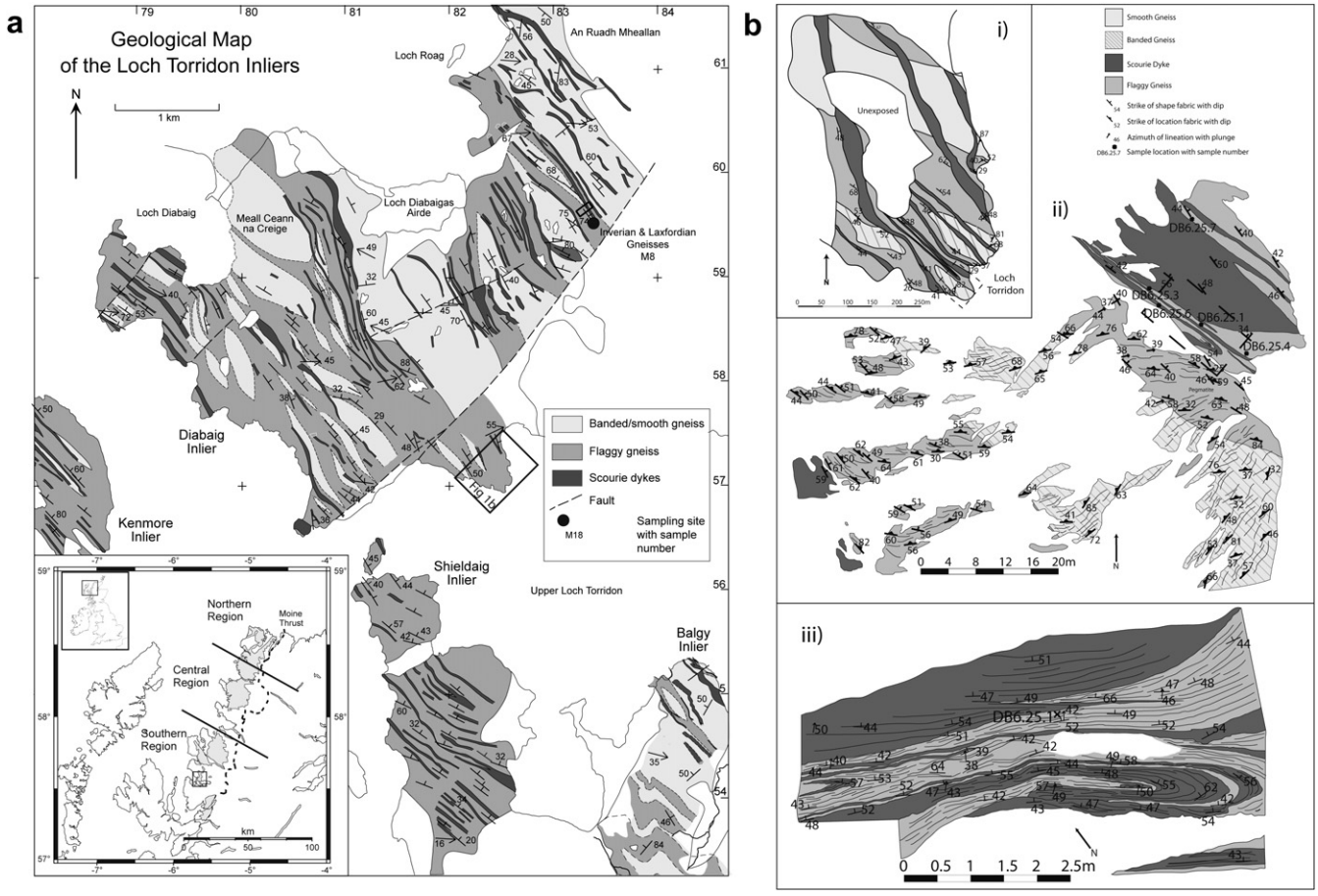


**Fig. 1.** Location map. a) Map of varying strain within Torridon high strain zone (from Wheeler, 2007). Torridon inliers are located in the Southern region of the Lewisian complex (grey shading, inset). b) i) Map of Alligin peninsula showing the relationship between dykes, high strain (flaggy) and low strain (banded, smooth) gneisses. ii) Outcrop map of the edge of a high strain zone exposed on the coast. iii) Detailed fabric map of the isoclinally folded Scourie dykes and interleaved gneisses. Form lines in ii) and iii) show location fabric which is parallel to shape fabric in high strain areas.

### 2.2. Field relations and sample descriptions

To the north of the Torridon high strain zone, undeformed dykes cut Badcallian location fabrics. Within the high strain zone deformed dykes contain an L-S shape fabric defined by amphibole grain shapes and plagioclase aggregate shapes. In larger dykes the strain is heterogeneous with anastomosing high strain zones cutting pseudomorphed igneous textures. In areas of more intense Laxfordian (post-dyke) strain a number of geometrical features suggest that the mafic dykes are weaker than the surrounding gneisses.

1) Folds developed where the lithologies are interleaved show the dykes forming cuspate protrusions into more rounded folds within the gneiss (Fig. 2a).
2) Isoclinally folded dykes show more thickening in their hinges than the felsic gneisses (Fig. 2b). The hinge to limb thickness ratio is ~7 for the mafic layers and 4 for the gneisses (Fig. 1c-iii).
3) Where dykes are intruded cross cutting older gneissic fabrics, subsequent shear has been localised in the dykes (Fig. 2c and d). If they were stronger than the gneisses then the gneisses would accommodate the strain and the dykes remain underformed.

In order to assess the deformation mechanisms active and the reason for the relative weakness of the mafic rocks, a number of different samples have been analysed from different parts of the Torridon high strain zone. Along the north shore of Loch Torridon (Fig. 1a), a series of Scourie dykes is exposed (Fig. 1b–i) showing pervasive shape fabric defined by hornblende grain shapes and plagioclase aggregates with minor isolated quartz. In the gneisses, feldspar-rich leucosomes were produced by migmatisation during both the Inverian and preceding high-grade events (Cresswell and Park, 1973). The age of these and folds which affect them is often ambiguous. However, in one locality a pair of Scourie dykes and interleaved gneisses have been folded isoclinally (Fig. 1b-ii, iii) and are exposed in the intertidal zone. This deformation is unequivocally Laxfordian in age as it folds not only the dyke-gneiss contact but also the hornblende and plagioclase aggregate shape fabric within the dyke. Thickening of the folded dykes around the fold hinge (Figs. 1b-ii, iii and 2b) suggests that the dykes are less competent than the surrounding gneisses. The mineral/mineral-aggregate stretching lineations in the dykes and gneisses are both parallel to the fold hinge (where visible) suggesting that the deformation was contemporaneous in the dykes and gneisses. The shear sense of this part of the high strain zone has been determined to be normal following the method of Wheeler (1987).

To assess the effect of increasing strain on the rock microstructure, samples of a deformed dyke (DB6.25.6) and gneiss from a single layer within the folded zone which changes thickness along its length were collected. Interpreting a reduction in thickness as an increase in strain, the samples increase in strain as follows DB6.25.3 > DB6.25.1 > DB6.25.4. With increasing strain (Fig. 3b – d) the banding present in the lower strain samples is thinned and destroyed leaving isolated porphyroclasts. Another sample (DB6.25.7, Fig. 3a) was collected which contains a large deformed leucosome layer and is treated as an example of even lower strain. In the lower strain (banded gneisses; Figure 1b-ii) areas the banding appears to be related to partial melting of uncertain age. In thin

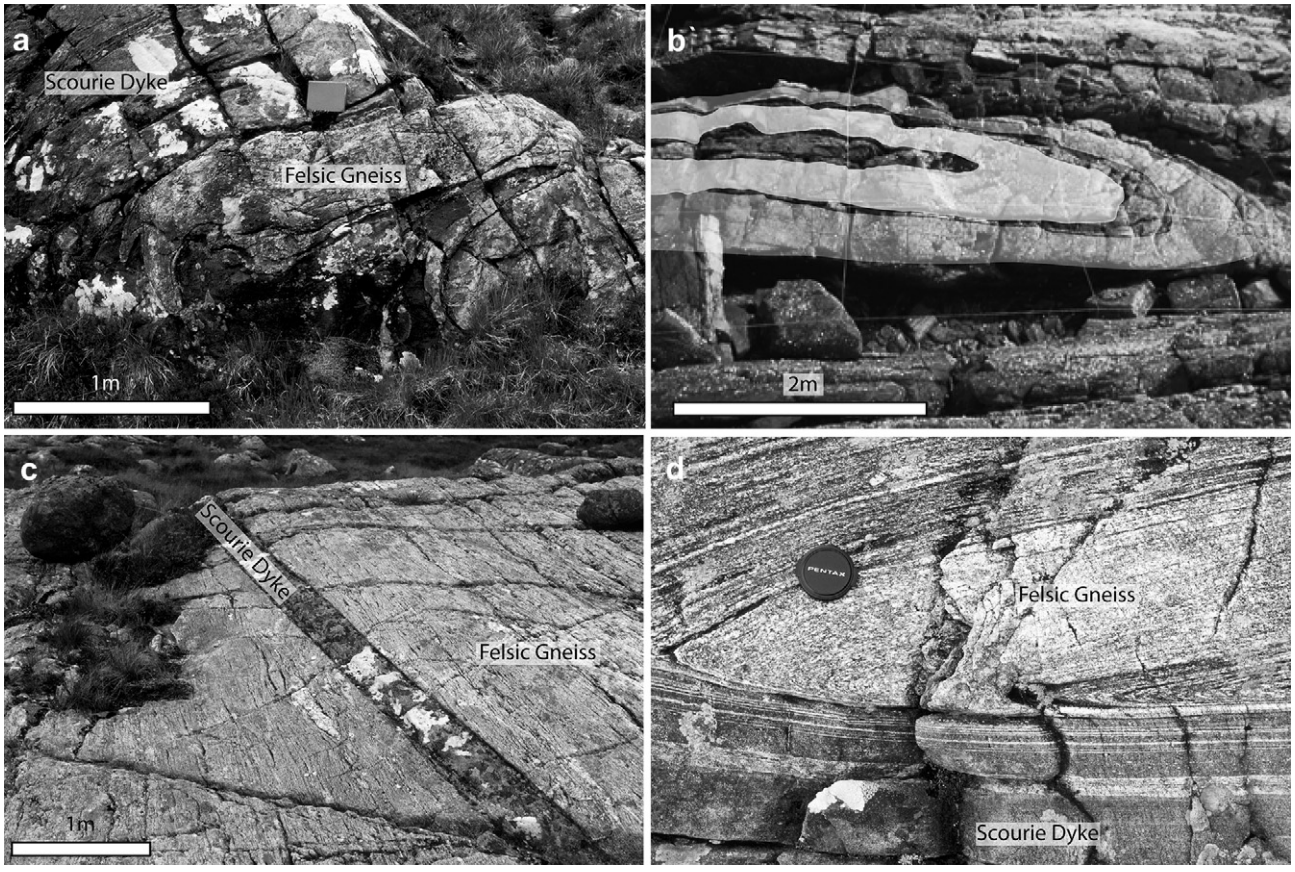


**Fig. 2.** Outcrop photos showing evidence for strength contrast between gneisses and dykes. a) Folded dykes within gneisses show cuspate geometries indicating dykes are weaker. b) Greater amount of thickening of a dyke around a fold hinge relative to the interleaved gneisses exposed on the shore at Alligin (Fig. 1b-iii) – dykes are shown by shading. c) and d) Dykes intruded obliquely to gneissic foliation show intense shape fabric development.

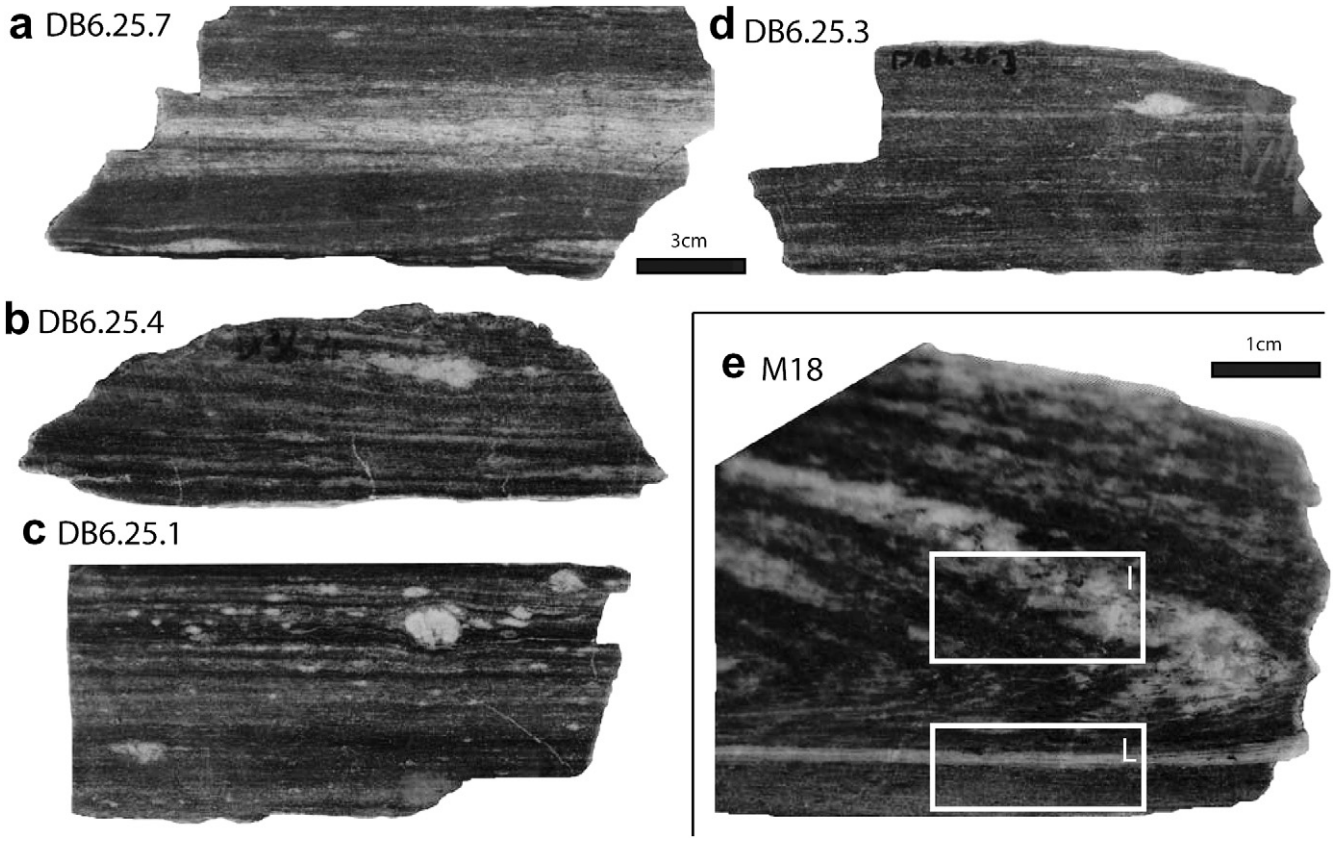


**Fig. 3.** Optically scanned images of samples cut parallel to kinematic X–Z plane. a) DB6.25.7, lowest strain gneiss with thick leucocratic band. b) DB6.25.4, banding is beginning to be boudinaged and homogenised. c) DB6.25.1, banding is largely homogenised leaving porphyroclasts. d) DB6.25.3, highest strain sample from Alligin. e) M18 showing fold formed by Laxfordian shearing of Inverian fabric. Two sections are taken from this sample, on with Inverian fabric (I) and one with Laxfordian fabric (L).

section these rocks are dominated by chemically zoned plagioclase, quartz and mica.

The mica content of the rocks varies greatly. In some samples, there is enough mica to form through-going bands on the scale of a thin section. In the rocks detailed in this study, the mica forms isolated grains and which do not form a load-bearing framework and therefore do not dominate the rheology of the rocks. The variation in mica content of the rocks may be caused by K-metasomatism during deformation or by variations in bulk composition within the shear zone. Studies of the effect of shearing on mineralogy and chemistry (Beach, 1976) at Torridon have shown that K was introduced during Inverian migmatisation but not during Laxfordian deformation. Since none of the samples examined here exhibit load-bearing frameworks of mica, it is still possible to examine the effects of increasing strain on deformation mechanisms because the mica cannot deform without deformation in the surrounding matrix.

Whilst deformation at Alligin is demonstrably Laxfordian in age, Inverian deformation is harder to identify. There are however a number of outcrops where there are shape fabrics which are discordant to dykes by ~20°. In one case (M18, Fig. 3e) Laxfordian deformation is localised along the margin of a dyke causing the location fabric to bend through ~160°; the fabric on the other limb of the 'bend-in' fold is Inverian. The microstructures of these two components differ in the grain size and distribution of phases. The Inverian part has large areas of plagioclase which has a grain size of >500 μm. The Laxfordian part has finer grained plagioclase (~300 μm) which is mixed with quartz and biotite. Zoning in the plagioclase has been interpreted to have resulted from post-deformation grain-recycling (Pearce and Wheeler, 2010).

### 2.3. Deformation conditions

Metamorphic conditions for the Torridon high strain zone are not well constrained because of the high variance mineral assemblage common in many metagranitic rocks. Temperature and pressure estimates for Laxfordian amphibolite facies metamorphism from the Loch Maree Group to the north are given as 630 ± 30 °C and 6.5 ± 1.5 k bar from metapelites (Droop et al., 1999). Temperatures and pressures for post-deformation grain growth, which causes plagioclase zoning, from Torridon are 590–610 °C during decompression from 9.3 to 7 k bar (Pearce, 2009). Deformation preceded this growth but there is no evidence for dramatically changed metamorphic conditions between the cessation of tectonism and the development of the chemical zoning. Consequently the starting temperature for the grain growth is inferred to represent deformation temperature and is consistent with those of Droop et al. (1999).

## 3. Electron backscatter diffraction (EBSD) methodology

This study uses electron backscatter diffraction (EBSD) to characterise rock microstructures and crystallographic fabrics (Prior et al., 1999, 2009). All data were collected from thin sections cut parallel to the profile (kinematic X–Z) plane, perpendicular to foliation and parallel to lineation. Following an outline of the operating conditions we give a description of the data collection strategies for the collection of different types of data

Electron backscatter diffraction was carried out on a Philips XL30 fitted with an HKL Nordlys EBSD camera at the University of Liverpool using an accelerating voltage of 20 keV, and beam current

~5 nA. Thin sections were chemically polished with SYTON colloidal silica, and coated with a thin carbon coat. EBSD patterns were indexed using the Channel 5 suite of programs from HKL-Oxford Instruments. Maps of representative microstructures were collected using step sizes on the order of 2–5% of the mean grain-diameter (5 μm for these rocks). These data as can be used to see the distribution of phases as well as the presence or lack of internal grain deformation which is used to infer deformation mechanisms. Following collection, these data were processed using the Tango module of the HKL EBSD suite using routines described by Bestmann and Prior (2003) and Prior et al. (2009).

EBSD was also carried out to collect crystallographic preferred orientations (CPOs) of gneiss and dyke samples. Step sizes similar to the grain size (250–300 μm) were used so that nominally only one point was collected per grain. This technique was used to collect statistically significant datasets efficiently. It is akin to creating EBSD maps then sampling one point per grain, ensuring that the CPO produced is not dominated by one large grain. In studies that investigate volume averaged properties (e.g. seismic anisotropy calculations), this one point per grain approach is inappropriate because large grains contribute more to the bulk property. In studies concerned with deformation mechanisms, it is necessary to sample a statistically significant number of grains with each contributing equally to the sample so that the resulting data are not swamped by one large grain. Recent studies have shown that it is possible to reliably index feldspars automatically (Mariani et al., 2009; McLaren and Reddy, 2009) with limited misindexing. However, the quality of these data was tested for two samples by manually indexing a subsample of patterns and comparing the outcome with the automated results. The bulk fabric data are contoured in multiples of a uniform distribution using the PFCh5 program, written by Prof. D. Mainprice, which also calculates the eigenvalues and vectors of the fabric ellipsoid. These are used to estimate the strength and shape of the fabric in terms of point, girdle, and random components (Vollmer, 1990). Plotting these components on a ternary plot allows relative fabric strength and shape to be easily seen.

## 4. Scourie dykes

Here we present EBSD data from Scourie dykes and interpret it in terms of the deformation mechanisms active during the deformation of the dykes.

### 4.1. EBSD Data

Three samples of deformed Scourie dykes were analysed for bulk CPO data. One was mapped to show the typical distribution of phases, shapes of grains, and internal misorientations within grains. In none of the cases examined here is it possible to calculate the strain accommodated by the samples but it is estimated that $\gamma > 10$ because the fabric is parallel with the margins of the dykes. Moreover, plagioclase aggregates are extremely strung out, in some cases to a single grain width, so it is not possible to estimate strain using the assumption that these are passive markers.

Hornblende forms a load-bearing framework with elongate grains parallel to the macroscopic lineation direction whilst the plagioclase and quartz grains show more equant grain shapes (Fig. 4a). None of the minerals show undulose extinction or sub-grains. Lack of distortion requires that there is no imbalance of dislocations of opposite sign and, given EBSD pattern quality is good, is best explained by low dislocation densities. This may be due to none being present in the original deformation (i.e. the rock deformed by diffusion creep), or subsequent annealing during the static grain growth event which has been identified in these rocks (Pearce, 2009). The plagioclase appears as lines of grains parallel with the foliation. It may be that they originated as a single recrystallised grain and have subsequently been drawn out into a single grain width layer.

Bulk fabric data were collected on a 300 μm grid over the entire thin section (~3 by 2 cm). Due to the grain-shape fabric in amphibole this may have resulted in more than one point per grain along the long axis of grains. Therefore, following acquisition, any adjacent points which were within 10° of each other were considered the same grain and only one of these was taken for the analysis. All of the dykes showed the same CPO; a representative sample is shown in Fig. 5.

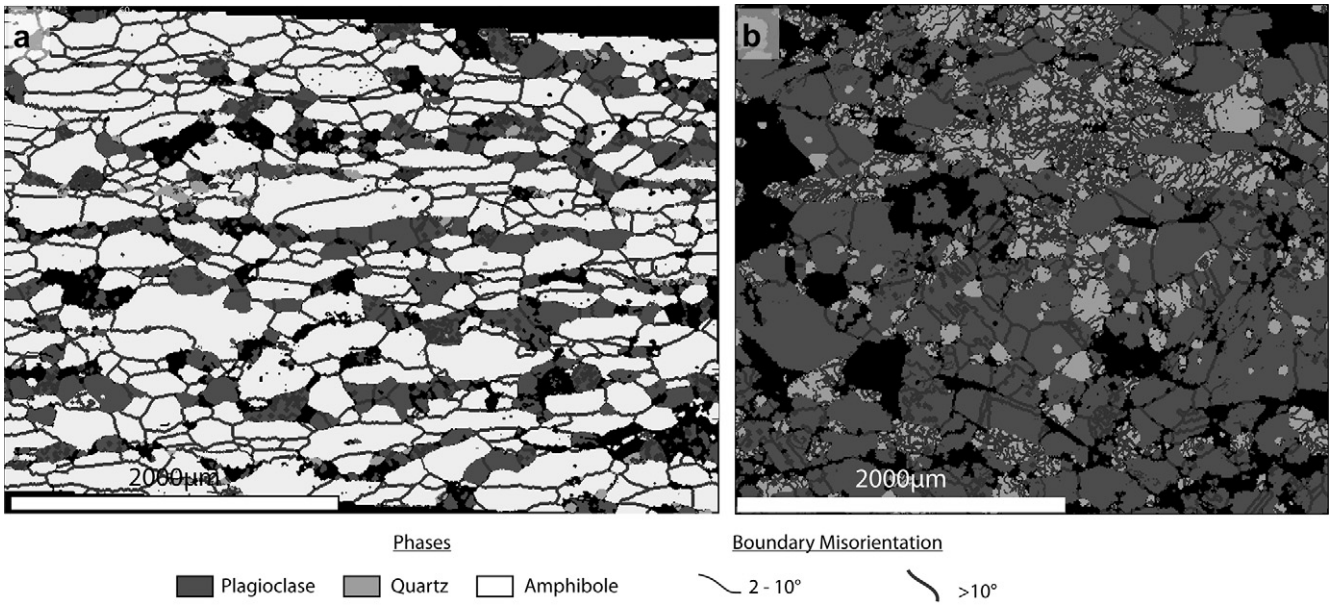


**Fig. 4.** Exemplar EBSD maps from a deformed Scourie dyke, DB6.25.6 (a) and a Laxfordian gneiss, DB6.25.1 (b). Pixels are coloured by phase and grain boundaries are overlain. Thicker grain boundaries are misorientations >10°, thinner grain boundaries are misoroentations of 2°–10°.

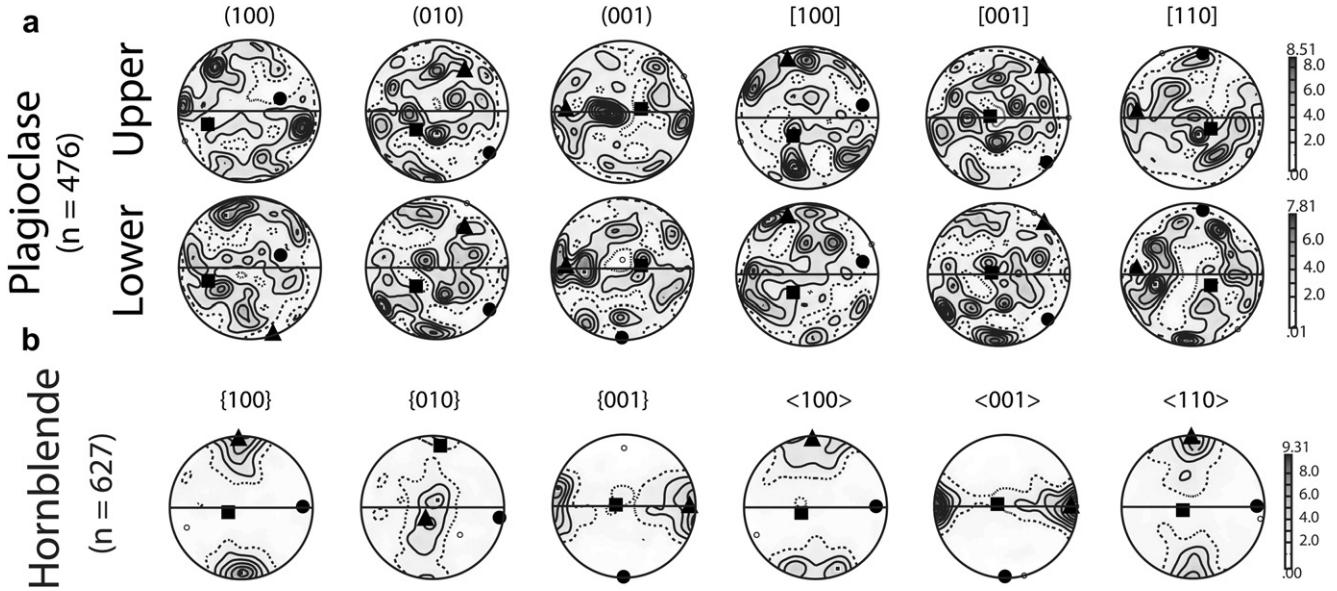


**Fig. 5.** Bulk fabric data from a Scourie dyke sample (DB6.25.6) from the limb of one of the isoclinal folds (Fig. 1b–iii). a) Plagioclase; both hemispheres are displayed due to the triclinic symmetry. b) Hornblende; shown as lower hemisphere plots. All figures are contoured with multiples of the mean uniform distribution. Data are one point per grain with the number of grains ($n$) given for each dataset. Eigenvectors $\lambda_1 > \lambda_2 > \lambda_3$ are displayed as triangle, square and circle respectively.

Plagioclase orientation data from deformed Scourie dykes (Fig. 5a) shows textures (Fig. 6a) which have no symmetry with respect to the kinematic reference frame. Therefore, these cannot be explained by the activation of dislocation slip systems. Hornblende (Fig. 5b) has a CPO with (100) parallel to the foliation and <001> aligned with the mineral and mineral aggregate stretching lineation. Both are between ideal girdle and single point distribution (Fig. 6a) but the poles to (100) are closer to a point and the [001] directions are closer to a girdle distribution.

### 4.2. Dyke deformation mechanisms

High temperature deformation of rocks in the crust is accomplished by volume constant creep facilitated by crystal plasticity (dislocation creep) with or without grain-boundary sliding, grain-boundary diffusion (Coble) creep or a combination of the two. Where dislocations are preserved the slip systems are identifiable by analysing lattice distortion using EBSD (Barrie et al., 2008; Hildyard et al., 2009; Wheeler et al., 2009). In the absence of preserved dislocations due to annealing, presence of a CPO may indicate that dislocation creep was once active. Whilst it is commonly assumed that diffusion creep does not produce a CPO, numerical models of diffusion creep with anisotropic dissolution and precipitation rates suggest that it may be possible to generate a CPO by diffusion creep deformation (Bons & den Brok, 2000) but this CPO may not be reconcilable with known slip systems in the mineral. When considering which deformation mechanisms were active, it is necessary to consider the temperature and pressure, grain size and water activity at the time of deformation. Post-tectonic grain growth has been inferred to begin at ~600 °C and 8–9 k bar (Pearce, 2009). These are assumed to be the deformation conditions. Compositionally

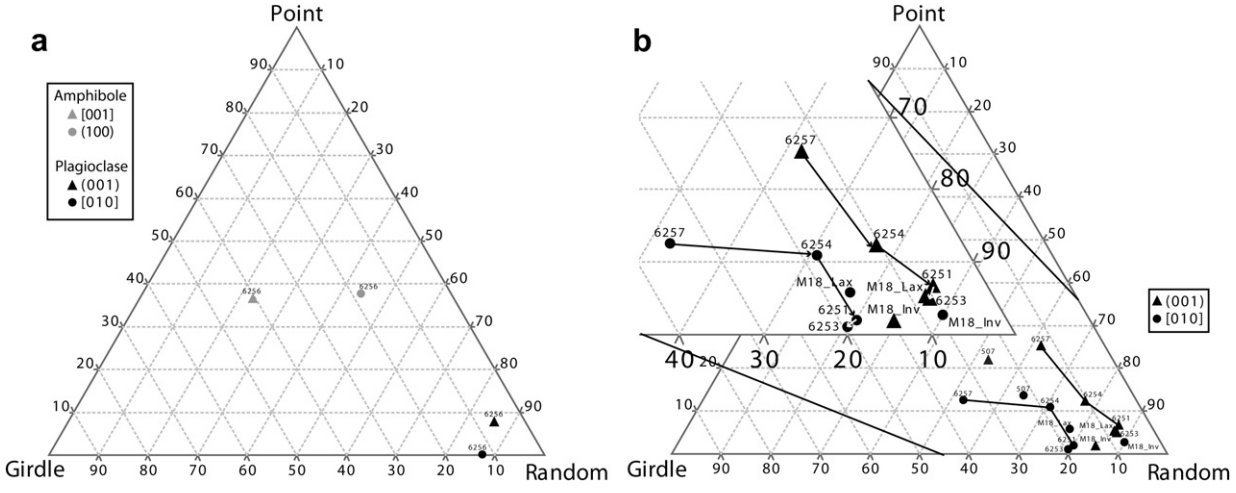


**Fig. 6.** Eigenvalue analysis of plagioclase and amphibole fabrics. Point, girdle and random components are calculated from the eigenvalues of the fabric ellipsoid. a) Plagioclase (black) and amphibole (grey) fabrics from deformed Scourie dykes. b) Plagioclase fabrics from gneisses plotted in terms of point, girdle and random components (after Vollmer, 1990). Points joined with a black line are the samples from Alligin joined in an up strain order.

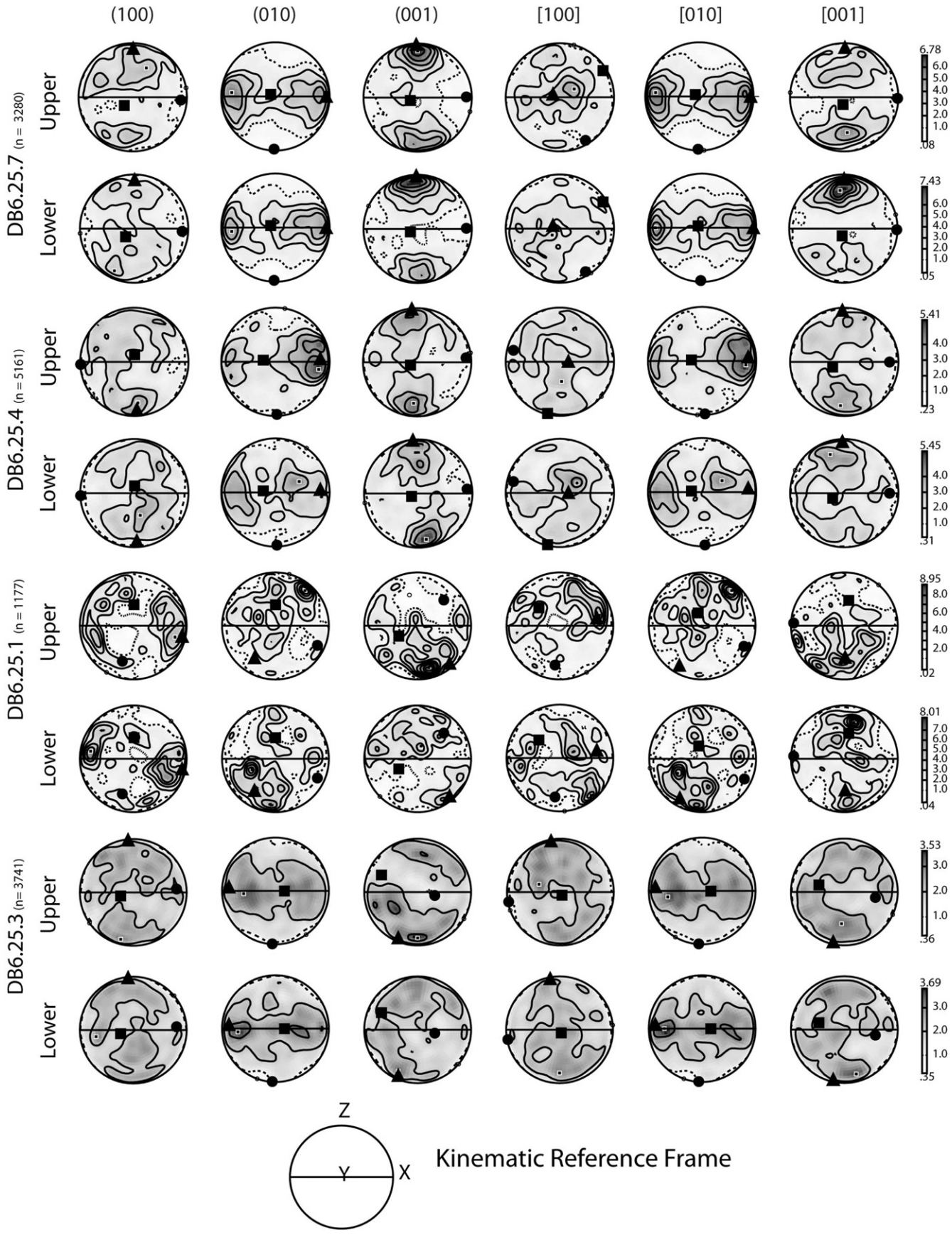
(100)
(010)
(001)
[100]
[010]
[001]
DB6.25.7 (n = 3280)
Upper
Lower
DB6.25.4 (n = 5161)
Upper
Lower
DB6.25.1 (n = 1177)
Upper
Lower
DB6.25.3 (n= 3741)
Upper
Lower
6.78
6.0
5.0
4.0
3.0
2.0
1.0
.08
7.43
6.0
5.0
4.0
3.0
2.0
1.0
.05
5.41
4.0
3.0
2.0
1.0
.23
5.45
4.0
3.0
2.0
1.0
.31
8.95
8.0
6.0
4.0
2.0
.02
8.01
7.0
6.0
5.0
4.0
3.0
2.0
1.0
.04
3.53
3.0
2.0
1.0
.36
3.69
3.0
2.0
1.0
.35
Z
Y
X
Kinematic Reference Frame

uniform cores of 50–100 μm are interpreted to represent the maximum pre-growth grain size in both the dykes and gneisses. Therefore, this is the inferred maximum grain size during deformation (Jessell et al., 2003).

#### 4.2.1. Plagioclase

Plagioclase CPOs from the Scourie Dykes cannot be interpreted simply in terms of dislocation slip systems. The current grain size is considerably less than would be expected in the unmetamorphosed dykes based on petrographic evidence from undeformed samples. Therefore, the plagioclase underwent grain size reduction between intrusion and the end of deformation. This may have occurred dynamically during deformation driven by strain or by chemically driven neocrystallisation. Strain-driven grain size reduction is often thought to result in a switch to grain size sensitive deformation mechanisms (e.g. Hobbs et al., 1990) however, such a switch has been questioned (De Bresser et al., 2001) and even if it does occur may not necessarily cause complete destruction of the existing CPO (Wheeler, 2009).

Chemically driven neocrystallisation causes extreme grain size reduction by nucleating new grains of a more stable composition at the expense of existing disequilibrium grains (Stünitz, 1998; Wayte et al., 1989). Jiang et al. (2000) showed that domainal CPOs can be produced where different areas of the rock have CPOs related to a single parent grain, but these CPOS are not related to the kinematic framework. This process may be active here but the plagioclase is mixed with the amphibole and therefore it is difficult to identify if multiple plagioclase grains came from the same parent. The grain size produced by chemically driven neocrystallization is much finer than predicted by piezometers (e.g. Post and Tullis, 1999) so more grain growth, longer times, and (at a constant strain rate) larger strains were achieved before dislocation creep became a significant deformation mechanism. Furthermore, undeformed dykes show pseudomorphing of igneous textures by plagioclase polycrystals suggesting that there was enough excess chemical energy in the original plagioclase composition to cause neocrystallisation.

#### 4.2.2. Amphibole

Amphiboles do not preserve evidence for lattice distortion by dislocations. This can be interpreted as either deformation by dislocation creep and subsequent annealing to remove dislocations or deformation by a mechanism other than dislocation creep. Hornblende has a CPO consistent with slip on the (100) plane with Burgers vector [001] in accordance with experimentally defined slip systems (Dollinger and Blacic, 1975). The von Mises criterion states that for homogeneous, volume constant deformation in three dimensions five slip systems are required to be active. It is difficult to assess whether the deformation is homogeneous, but there does not appear to be any localisation of strain in a particular phase, which may relax this criterion. If the deformation is homogeneous then (100)[001] cannot be the only slip system but may be the dominant one. The activity of grain-boundary sliding relaxes the von Mises criterion and slip can be accommodated on a single slip system (Goldsby and Kohlstedt, 1997), the disGBS mechanism (Hirth and Kohlstedt, 2003). This slip system will be the one with the lowest critical resolved shear-stress. In this case the (100)[001] would be interpreted as the 'easiest' slip system. Whilst plasticity on this slip system has been observed experimentally (Dollinger and Blacic, 1975) in synthetic aggregates, experiments on natural amphibolites with 50% amphibole and 50% plagioclase (Hacker and Christie, 1990) show that deformation of amphiboles is cataclastic up to and exceeding 750 °C even at confining pressures >1 GPa. Furthermore, naturally deformed amphibolites analysed by EBSD (Aspiroz et al., 2007) show similar CPOs but lack any evidence for crystal plastic deformation at temperatures over 100 °C above those inferred for the deformation of the Scourie dykes. The samples of Aspiroz et al. (2007) were interpreted to have deformed by rigid rotation of elongate amphibole grains in a less viscous plagioclase matrix. However, this is not a viable deformation mechanism for these rocks because the amphibole forms the load-bearing framework (Handy, 1990) thereby precluding rigid rotation.

It is proposed that the amphibole CPO formed by dissolution-precipitation creep of fine-grained amphibole aggregates. Whilst it is generally considered that grain size sensitive deformation does not produce a CPO, numerical modelling (Bons & den Brok, 2000) has suggested that it may be possible in minerals that have anisotropic dissolution and growth rates. Given the extreme elastic anisotropy of amphiboles and elongate grain in igneous rocks, it is likely that amphibole also has anisotropic growth rates. Prior to the growth, grain size reduction may have occurred by cataclasis or chemically driven recrystallisation. However, a comparison of deformed and undeformed amphibole chemistry from Scourie dykes (Pearce, 2009) shows that deformation has homogenised amphibole compositions. This is consistent with the grain size reduction being chemically driven as fracturing would not necessarily change mineral chemistry. Dissolution-precipitation creep has been shown to be active in rocks deformed at similar conditions (Wintsch and Yi, 2002) and often to result in mineral zoning. However, zoning would only occur if the stable mineral composition was changing over time. Therefore the absence of mineral zoning does not preclude solution-precipitation creep as a deformation mechanism.

## 5. Quartzo-feldspathic gneisses

### 5.1. EBSD data

Gneisses were analysed by indexing plagioclase and quartz for both grain-scale maps and bulk CPOs. Plagioclase principal directions are plotted to give an idea of the degree of preferred orientation in each sample (Fig. 7). Common slip systems identified in plagioclase include (010)[001] and (010)[100] (Mehl and Hirth, 2008; Stünitz et al. 2003) so activity of these systems should be apparent from the principal directions.

A phase map of a large section of the microstructure of DB6.25.1 (Fig. 4b) shows a typical example of the distribution of quartz and plagioclase within the gneisses. Whilst some quartz aggregates form layers on the order of 4 mm long, there are also large areas with quartz grains isolated within a plagioclase matrix. Plagioclase grains show little internal distortion (few sub-grain boundaries), and no deformation twinning whilst quartz grains are filled with low angle (2°–10°) sub-grain boundaries and dauphine twins (Fig. 4). If the quartz deformation occurred in the amphibolite facies prior to the plagioclase grain growth, then it would have likely recovered and annealed as the plagioclase grew. Therefore the lattice distortion in the quartz is interpreted to have occurred during late stage greenschist facies deformation, and it will not be considered further.

**Fig. 7.** Plagioclase bulk fabric data from Alligin series gneisses. Finite strain magnitude increases from top to bottom which corresponds with a weakening in the preferred orientation seen in (001) and [010]. Data are one point per grain with the number of grains ($n$) given for each dataset. Contours are in multiples of the uniform distribution. Eigenvectors $\lambda_1 > \lambda_2 > \lambda_3$ are displayed as triangle, square and circle respectively.

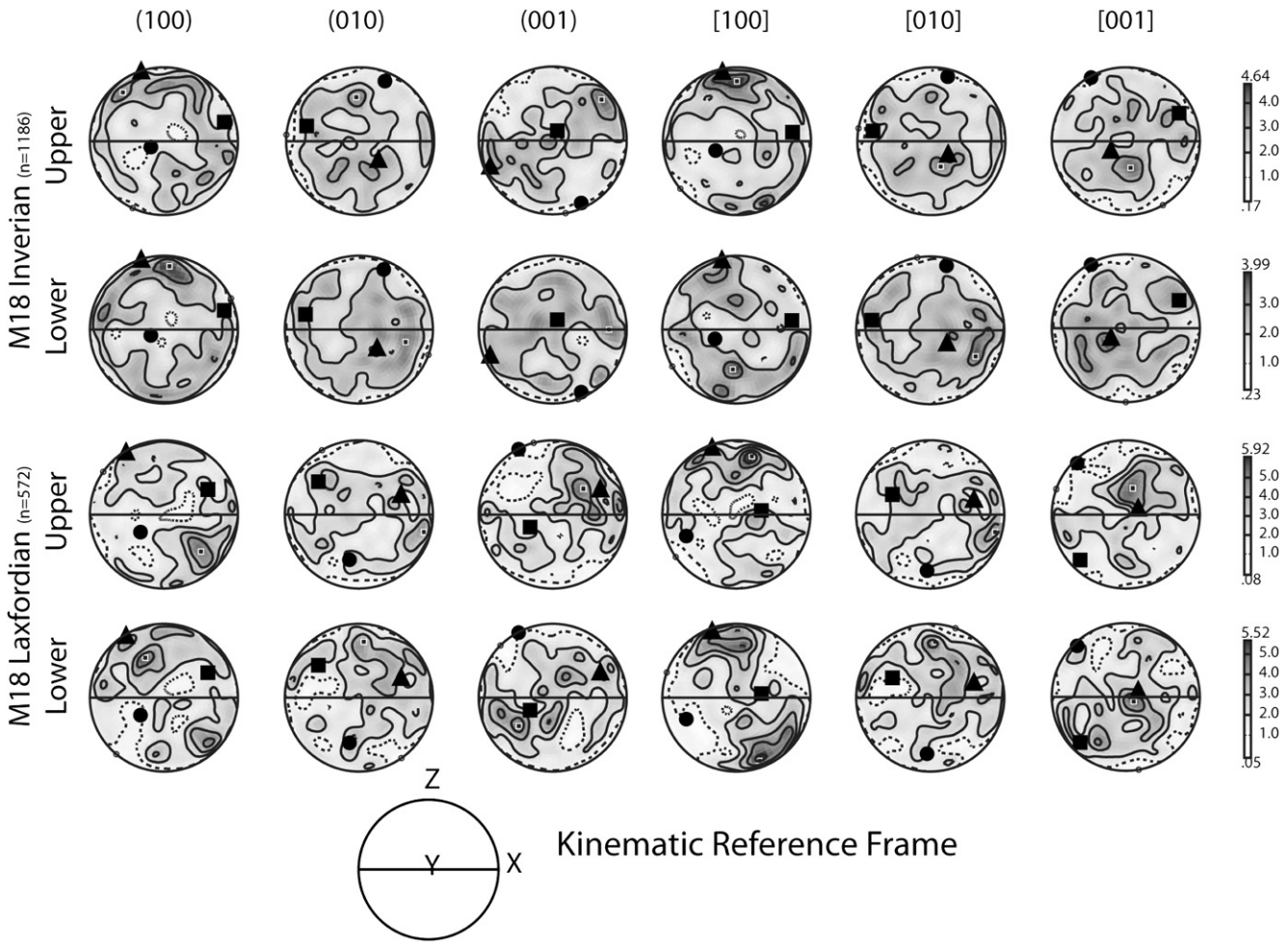


**Fig. 8.** Plagioclase bulk fabric data from both Inverian and Laxfordian part of M18 gneisses. M18 is plotted relative to the Laxfordian reference frame for both samples. Data are one point per grain with the number of grains ($n$) given for each dataset. Contours are in multiples of the uniform distribution. Eigenvectors $\lambda_1 > \lambda_2 > \lambda_3$ are displayed as triangle, square and circle respectively.

Bulk CPO data for plagioclase in the deformed gneisses (Figs. 7 and 8) show a variety of patterns which vary in both 'strength' and symmetry with respect to the kinematic reference frame. Fabrics from the Alligin series (6.25.1, 3, 4, and 7) show strong CPOs (Fig. 7) at lower strains (6.25.7) with point-maxima in the (001) pole figure, close to parallel with kinematic − Z, and point-maxima to girdle distributions in the [010] pole figures close to parallel with kinematic − X. These decrease in strength with increasing strain (i.e. show an increasing random component − compare DB6.25.7 and DB625.3 on Fig. 6b). Both Inverian and Laxfordian parts of M18 show complex CPOs which have no obvious single maxima or girdles (Fig. 6b).

The patterns seen in DB6.25.7, and DB6.25.4 could be explained by slip on the (001) plane in the [010] direction. However, [010] is a long Burgers vector in plagioclase and therefore is not favourable for dislocation slip because dislocations would have a large Peierls stress (Poirier, 1985 equation 2.59). Marshall and McLaren (1977a) defined the possible Burgers vectors based on geometrical criteria. These have been analysed for the samples with the strongest CPOs and the best ones shown here (Fig. 9a). In order to identify which of these possible vectors aligns best with the lineation, the data are viewed along the lineation so that the best fit clusters around the centre of the pole figure. DB6.25.4 shows clustering of [110] and DB6.25.7 shows clustering of [110] and $[1\bar{1}0]$ directions around the centre of the pole figure. This is consistent with other samples that have been analysed but are not shown. These directions are contained in a number of rational planes. Once again the best fit slip plane options are shown for DB6.25.4 and DB6.25.7. These data are rotated so that the direction of interest (the kinematic-Z direction in this case) is in the centre of the stereogram (which shows a view onto the X–Y plane with X at the E–W position). For DB6.25.7 (112) has the strongest maximum parallel with kinematic-Z. DB6.25.4 is less clear and the slip plane may be any of the planes presented. Plotting the planes in a crystal reference (Fig. 10c-i) frame shows the spatial relationship of the postulated slip systems. Both slip directions [110] and $[1\bar{1}\ 0]$ are contained in the (001) plane. Rotating the planes and directions shows the effect of aligning a crystal for slip on (112) $[1\bar{1}\ 0]$ (Fig. 10c-ii). The other possible slip planes are all very close in orientation so aligning one will produce a clustering of the others. However, it can be seen from DB6.25.7 (Fig. 10a) that the other planes produce more distributed maxima. The directions, [110] and $[1\bar{1}0]$ are not close to each other and therefore slip on one will not produce a clustering of the other close to it, thus allowing better discrimination between alternatives. Given the differences between postulated slip directions for different samples and the need for multiple slip systems according to the von Mises criterion it is likely that all of $(112)[1\bar{1}0]$, $(1\bar{1}2)[110]$, $(001)[1\bar{1}0]$, and $(001)[1\bar{1}0]$ are active but dominated to varying degrees by $(112)[1\bar{1}0]$ slip.

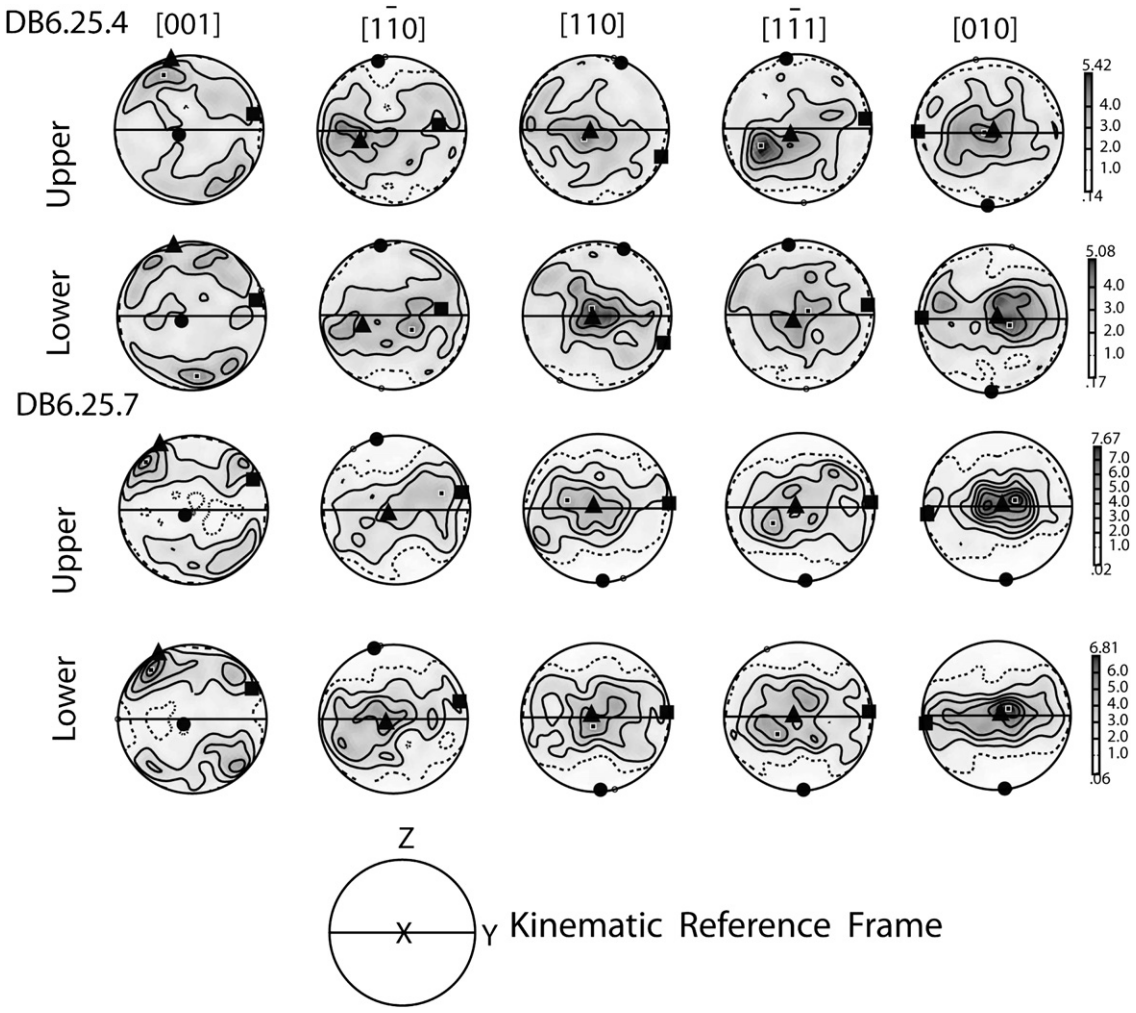


**Fig. 9.** Plagioclase fabrics viewed down the lineation. Fabrics were plotted for all possible Burgers vectors as defined by Marshall and McLaren (1977b) and [010] as a comparison and the best fit ones are shown. Data are viewed down the lineation so that the slip direction clusters in the centre of the stereogram making comparison easier. Data plotted are the same as Fig. 7 and are contoured in multiples of the uniform distribution.

### 5.2. Deformation and metamorphism in the gneisses

Orientation data from the gneisses can be divided into two subsets, Alligin Series and M18, which are used to examine the effects of strain on CPO and the difference between Inverian and Laxfordian microstructures, respectively.

#### 5.2.1. Alligin series

Plagioclase in Laxfordian gneisses from Alligin shows variable development of a CPO which is symmetrical with respect to the kinematic reference frame. The geometry of the CPOs is best explained through deformation by dislocation creep on a combination of $(112)[1\bar{1}0]$, $(1\bar{1}2)[110]$, $(001)[1\bar{1}0]$, and $(001)[1\bar{1}0]$. These Burgers vectors are the same length as the commonly observed [001] and therefore as likely (Marshall and McLaren, 1977b). Using the inference that layer thickness (of gneissic layers within the fold) is inversely proportional to strain, the strength of the CPO, characterised by the eigenvalue analysis, decreases with strain. It is hypothesised that the rocks deformed by dislocation creep initially and the grain size was reduced by dynamic recrystallisation. Deformation continued by diffusion creep accompanied by grain-boundary sliding which weakened but did not completely destroy the CPO, a possibility suggested by numerical modelling (Wheeler, 2009). Further evidence for the activity of diffusion creep and grain-boundary sliding is the destruction of the leucocratic banding, present in the samples from the thick part of the layer, which is progressively boudinaged and drawn out leaving only several large porphyroclasts (Fig. 3). At the microstructural scale quartz and plagioclase grains became mixed as opposed to the two minerals being present in monophase aggregates. Following strain-driven grain size reduction of plagioclase and quartz, the refined material gradually became more mixed with increasing strain accommodated by diffusion creep.

#### 5.2.2. M18 – Inverian and Laxfordian deformation

Neither the Inverian nor the Laxfordian sample from M18 shows a CPO which is symmetrical with respect to the Laxfordian kinematic reference frame. In the Laxfordian part this may result from superimposed deformations (Inverian followed by Laxfordian) which do not share symmetry elements and result in 'triclinic' fabrics. The differences between fabrics in M18 and the Alligin rocks can be explained by considering the histories of the two sets of samples.

The plagioclase in the Inverian part of M18 underwent Laxfordian recrystallisation driven by a combination of a small amount of strain and chemical disequilibrium which would have weakened or destroyed any Inverian CPO even without Laxfordian deformation. The Laxfordian part of M18 would also have undergone Laxfordian

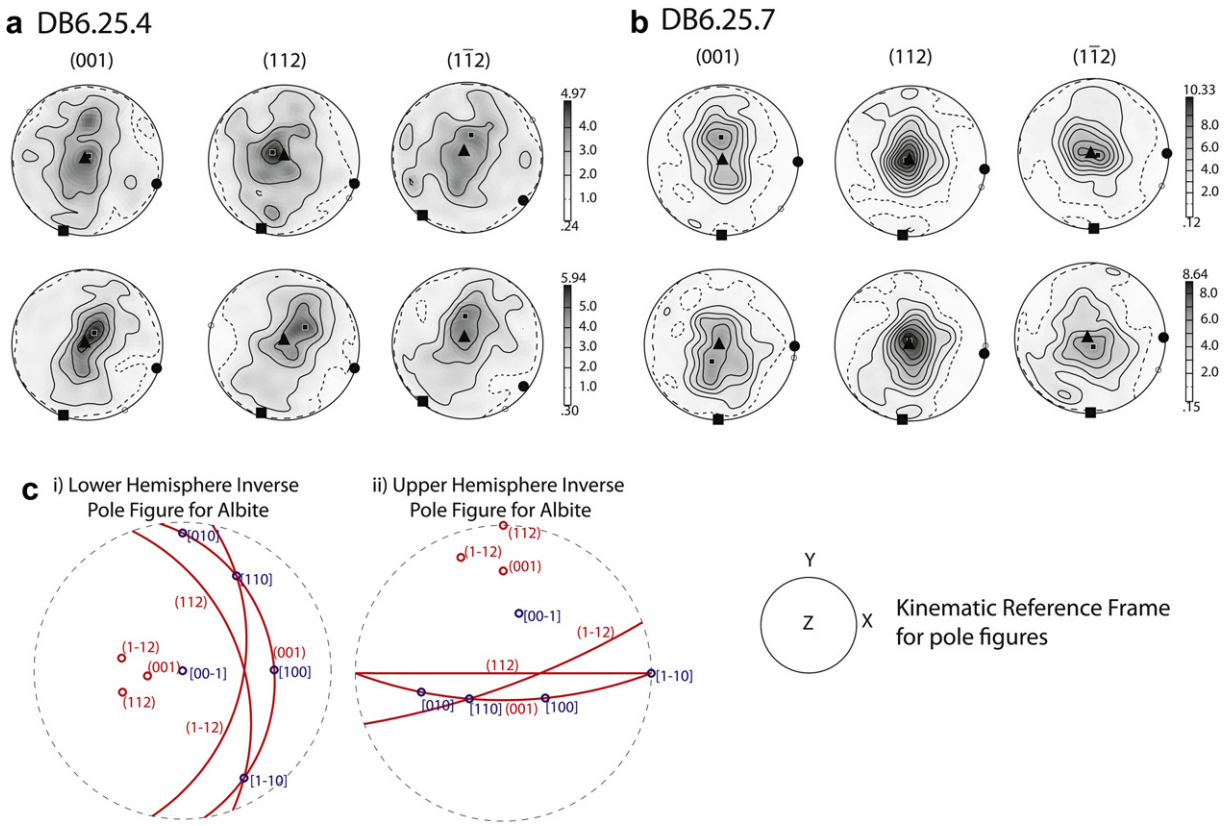


**Fig. 10.** Plagioclase fabrics viewed onto the kinematic X–Y plane with the same number of points as Fig. 7a–b) Rational planes which contain [110], and $[1\bar{1}0]$ plotted for samples with a CPO symmetrical with the kinematic reference frame. Pole to foliation is in the centre of the stereogram so that planes which are close in orientation can be easily distinguished. Pole figures contoured with multiples of the uniform distribution. c) Inverse pole figures showing the planes plotted and the inferred slip directions in crystallographic co-ordinates (i) and rotated so that $[1\bar{1}0]$ is parallel with the lineation and (112) is parallel with the foliation (ii).

recrystallisation driven by the same forces as the Inverian part thereby reducing the plagioclase grain size without deformation. Quartz grain size would have been reduced by dynamic recrystallisation. Following grain size reduction of both phases, further deformation accompanied by grain-boundary sliding destroyed the coarse Inverian banding and resulted in phase mixing at the microstructural scale in the Laxfordian part of M18. In the Inverian part, no strain was accommodated and therefore there was no phase mixing so the grains were able to grow to larger grain sizes following deformation. Therefore the lack of plagioclase CPO in M18 can be ascribed to the lack of dislocation creep deformation because the rocks underwent grain size reduction dominated by chemical disequilibrium. This model also accounts for the differences in distribution of phases between Inverian and Laxfordian part of the sample.

## 6. Rheological evolution of amphibolite facies rocks

Deformation mechanisms active in the major rock forming minerals of the TTG gneisses and Scourie dykes have been investigated using EBSD. Although rock microstructures have been altered by post-tectonic grain-recycling, different samples preserve a variety of deformation fabrics. Plagioclase undergoes a dramatic change in rheology throughout the amphibolite facies (Rybacki and Dresen, 2004) where both dislocation and grain-boundary diffusion creep can accommodate strain depending on the grain size. In rocks from the Lewisian gneiss, CPOs which are symmetric with respect to the kinematic reference frame, are inferred to have resulted from dynamic recrystallisation at ~600 °C. Subsequent deformation accompanied by grain-boundary sliding at the same conditions weakened the previously developed CPOs. Initial development of CPOs was governed by the starting microstructure. Samples with leucocratic banding, resulting from Inverian partial melting (Cresswell and Park, 1973), contained coarse-grained plagioclase which deformed by dislocation creep (Fig. 11 Alligin). Other samples containing Inverian fabrics underwent grain size refinement dominated by chemically driven processes so that no CPO was produced (Fig. 11 M18). This resulted from disequilibrium plagioclase compositions at the beginning of the Laxfordian. However, only Inverian samples close to Laxfordian deformation (M18) experience this process so a small amount of strain and fluid may have been required to drive recrystallisation. In this case the grains have no CPO because chemically driven nucleation of new grains is the dominant driving force rather than strain-driven subgrain rotation or grain-boundary bulging.

Grain size refinement in the dykes contrasts with the gneisses. This occurred during early Laxfordian metamorphism of the original igneous assemblage to hornblende schist. Since the same retrogression affected the undeformed dykes this is completely driven by reduction in Gibbs free energy. Fine-grained plagioclase aggregates then deformed by diffusion creep as the grain size is extremely small following metamorphism (Fig. 11 Dykes). Even taking into account the effects of syntectonic grain growth, which reduces the strain rate as the grain size increases, strains of >100 can be accumulated at 600 °C in the absence of a significant proportion of dislocation creep. Although amphibole fabrics are consistent with deformation by dislocation creep on (100) [001] comparison with other studies of both naturally and experimentally deformed amphibolites (Aspiroz et al., 2007; Hacker, 1990; Nyman et al., 1992) suggests that dislocation creep would

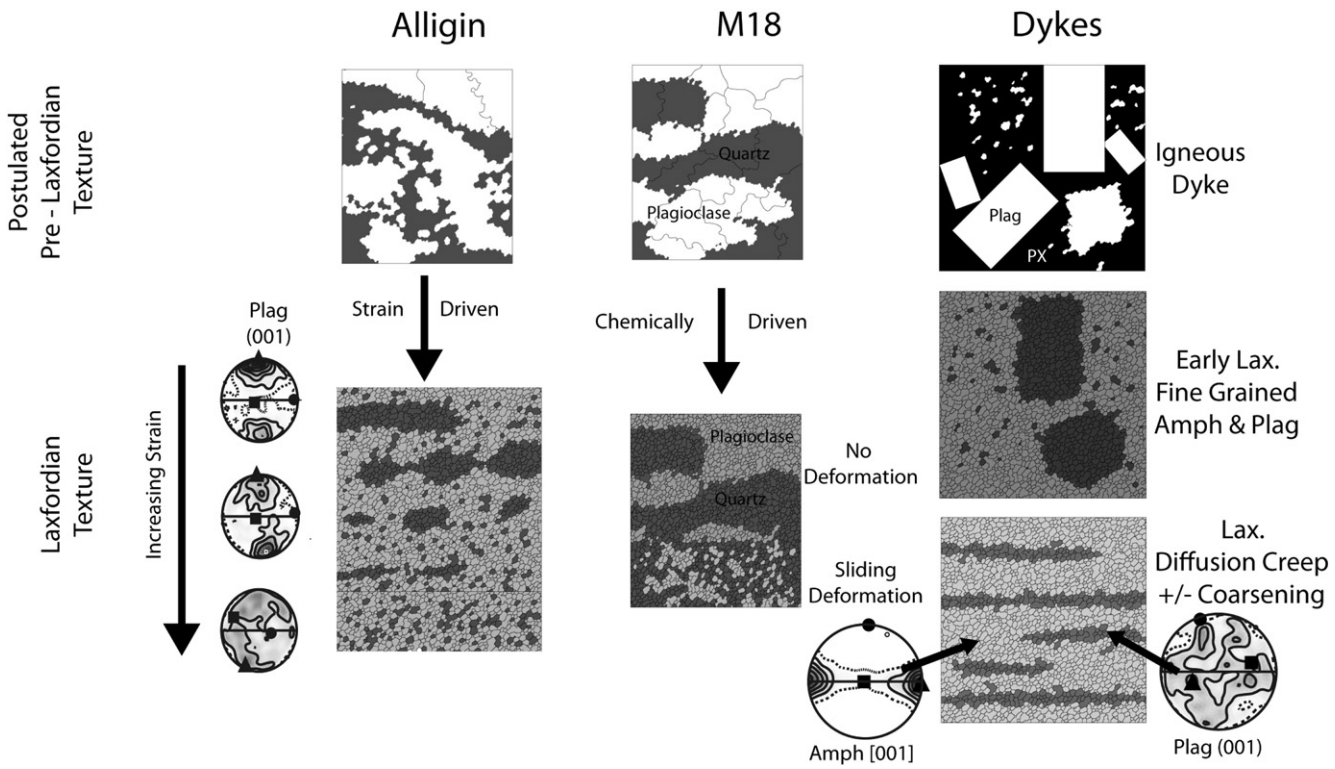


**Fig. 11.** Summary of microstructural evolution of different lithologies from Torridon. Alligin undergoes partial melting then strain-driven recrystallisation during the Laxfordian. Grain-boundary sliding causes phase mixing and weakening of plagioclase CPOs with increasing strain. M18 undergoes chemically-dominated recrystallisation and grain-boundary sliding so no CPOs are generated. Dykes are metamorphosed to fine-grained aggregates then undergo deformation by diffusion creep and grain-boundary sliding. Amphibole generates a CPO possibly due to later dislocation creep or anisotropic dissolution rates and plagioclase has no CPO.

not be the major strain accommodating mechanism under lower amphibolite facies conditions. It has been shown (Imon et al., 2004) that amphibole deforming by solution-precipitation creep under uppermost greenschist facies conditions can form a similar CPO to those observed here. It is more likely dissolution-precipitation creep would be dominant and that the necessary grain size reduction occurred either by cataclastic deformation (Aspiroz et al., 2007; Nyman et al., 1992) or neocrystallisation during metamorphism of the original dolerite (Brodie and Rutter, 1987).

Amphibole is considered to be strong under lower amphibolite facies conditions relative to plagioclase and quartz. However if both the gneisses and dykes are deforming by grain size sensitive processes then this assumption is not necessarily true. Imon et al. (2002) suggested that amphibolites deforming by solution-precipitation creep at 510 °C were equivalent in strength to quartz deforming by dislocation creep under similar conditions. Grain size reduction of plagioclase and hornblende in the dykes is due to chemically driven processes (or cataclasis) and was therefore likely to be extreme because the grains are formed as nuclei. Conversely, in the gneisses grain size reduction was achieved by dynamic recrystallisation so that the recrystallised grains are larger. Even allowing for subsequent grain growth of the fine-grained material in the dykes, the dykes would be weaker for a considerable length of time. This is consistent with the geometries of folds seen at Alligin and the observations of Wheeler et al. (1987) that Laxfordian strain is localised in the Scourie dykes.

## 7. Conclusion

Analysis of microstructures and crystallographic fabrics in polymineralic amphibolite facies rocks has highlighted the following points:

1) Data from amphibole show a CPO consistent with dislocation creep dominated by (100)[001] but no internal deformation is preserved. Fine-grained amphibole resulted from hydration of two-pyroxene dolerites and subsequent diffusion creep with anisotropic dissolution and precipitation rates may also produce the same CPO.
2) Plagioclase from the Scourie dykes has no CPO. This results from grain size reduction during metamorphism and subsequent diffusion creep.
3) Plagioclase from the gneisses shows variable development of CPO which is symmetrical with the kinematic reference frame. Plagioclase, dominantly within banding produced by Inverian partial melting, is deformed by dislocation creep on the $(112)[1\bar{1}0]$, $(1\bar{1}2)[110]$, $(001)[1\bar{1}0]$, and $(001)[1\bar{1}0]$ slip systems. With increasing strain this CPO is destroyed and the quartz and plagioclase are mixed by diffusion creep deformation accompanied by grain-boundary sliding.
4) Sliding processes are also important in rocks such as M18 which have experienced grain size refinement dominated by reduction of chemical energy. In these rocks the change in distribution of phases and lack of CPO attest to the active deformation mechanism.
5) Mafic rocks can be weaker than metagranitoids at amphibolite facies when the grain size is finer. The relative strengths are a function not only of mineralogy (governed by bulk composition) but of the metamorphic and deformation histories of the two lithologies.

This study highlights the importance of chemical reactions for grain size reduction in the crust. Fine grain sizes, formed by nucleation, cause rocks to be weaker than may be expected under prevailing conditions.

## Acknowledgements

This work was carried out during the tenure of a University of Liverpool Studentship (MAP). We thank reviewers Brad Hacker and Paul Bons for reviews which improved the paper.

## References

Aspiroz, M.D., Lloyd, G.E., Fernandez, C., 2007. Development of lattice preferred orientation in clinoamphiboles deformed under low-pressure metamorphic conditions. A SEM/EBSD study of metabasites from the Aracena metamorphic belt (SW Spain). Journal of Structural Geology 29 (4), 629–645.

Barrie, C.D., Boyle, A.P., Cox, S.F., Prior, D.J., 2008. Slip systems and critical resolved shear stress in pyrite: an electron back-scatter diffraction (EBSD) Investigation. Mineralogical Magazine 72 (6), 1181–1199.

Beach, A., 1976. The Interrelations of fluid transport, deformation, geochemistry and heat flow in early Proterozoic shear zones in the Lewisian complex. Philosophical Transactions of the Royal Society of London A 280. 569–604.

Bestmann, M., Prior, D.J., 2003. Intragranular dynamic recrystallization in naturally deformed calcite marble: diffusion accommodated grain boundary sliding as a result of subgrain rotation recrystallization. Journal of Structural Geology 25 (10), 1597–1613.

Bons, P.D., den Brok, B., 2000. Crystallographic preferred orientation development by dissolution-precipitation creep. Journal of Structural Geology 22 (11–12), 1713–1722.

Brodie, K.H., Rutter, E.H., 1987. The role of transiently fine-grained reaction-products in syntectonic metamorphism – natural and experimental examples. Canadian Journal of Earth Sciences 24 (3), 556–564.

Coward, M.P., 1984. Major shear zones in the Precambrian crust; examples from NW Scotland and southern Africa and their significance. In: Kroner, A., Greiling, R. (Eds.), Precambrian Tectonics Illustrated. E. Schweizerbart'sche Verlagsbuchhandlung, Stuttgart, pp. 207–234.

Cresswell, D., Park, R.G., 1973. The metamorphic history of the Lewisian rocks of the Torridon area in relation to that of the remainder of the southern Laxfordian belt. The Early Precambrian of Scotland and Related Rocks of Greenland, pp. 77–83.

De Bresser, J.H.P., Ter Heege, J.H., Spiers, C.J., 2001. Grain size reduction by dynamic recrystallization: can it result in major rheological weakening? International Journal of Earth Sciences 90 (1), 28–45.

Dollinger, G., Blacic, J.D., 1975. Deformation mechanisms in experimentally and naturally deformed amphiboles. Earth and Planetary Science Letters 26 (3), 409–416.

Droop, G.T.R., Fernandes, L.A.D., Shaw, S., 1999. Laxfordian metamorphic conditions of the Palaeoproterozoic Loch Maree Group, Lewisian complex, NW Scotland. Scottish Journal of Geology 35 (1), 31–50.

Evans, C.R., 1965. Geochronology of the Lewisian basement near Lochinver, Sutherland. Nature (London) 207 (4992), 54–56.

Goldsby, D.L., Kohlstedt, D.L., 1997. Grain boundary sliding in fine-grained Ice I. Scripta Materialia 37 (9), 1399–1406.

Hacker, B.R., 1990. Amphibolite-facies-to-granulite-facies reactions in experimentally deformed, unpowdered amphibolite. American Mineralogist 75 (11–12), 1349–1361.

Hacker, B.R., Christie, J.M., 1990. Brittle/ductile and plastic/cataclastic transitions in experimentally deformed and metamorphosed amphibolite. Geophysical Monograph 56.

Handy, M.R., 1990. The solid-state flow of polymineralic rocks. Journal of Geophysical Research 95, 8647–8661.

Hildyard, R.C., Prior, D.J., Faulkner, D.R., Mariani, E., 2009. Microstructural analysis of anhydrite rocks from the Triassic Evaporites, Umbria-Marche Apennines, Central Italy: an insight into deformation mechanisms and possible slip systems. Journal of Structural Geology 31 (1), 92–103.

Hirth, G., Kohlstedt, D.L., 2003. Rheology of the upper mantle and the mantle wedge: a view from the experimentalists. In: Eiler, J. (Ed.), Inside the Subduction Factory. Geophysical Monograph, 138, pp. 83–105. American Geophysical Union.

Hirth, G., Tullis, J., 1992. Dislocation creep regimes in quartz aggregates. Journal of Structural Geology 14 (2), 145–159.

Hobbs, B.E., Muhlhaus, H.B., Ord, A., 1990. Instability, softening and localization of deformation. In: Knipe, R.J., Rutter, E.H. (Eds.), Deformation Mechanisms, Rheology and Tectonics. Geological Society, London, Special Publications, vol. 54, pp. 143–166.

Imon, R., Okudaira, T., Fujimoto, A., 2002. Dissolution and precipitation processes in deformed amphibolites: an example for the ductile shear zone of the Ryoke metamorphic belt, SW Japan. Journal of Metamorphic Geology 20 (3), 297–308.

Imon, R., Okudaira, T., Kanagawa, K., 2004. Development of shape- and lattice-preferred orientations of amphibole grains during initial cataclastic deformation and subsequent deformation by dissolution–precipitation creep in amphibolites from the Ryoke metamorphic belt, SW Japan. Journal of Structural Geology 26, 793–805. doi:10.1016/j.jsg.2003.09.004.

Jessell, M.W., Kostenko, O., Jamtveit, B., 2003. The preservation potential of microstructures during static grain growth. Journal of Metamorphic Geology 21 (5), 481–491.

Jiang, Z., Prior, D.J., Wheeler, J., 2000. Albite crystallographic preferred orientation and grain misorientation distribution in a low-grade mylonite; implications for granular flow. Journal of Structural Geology 22 (11–12), 1663–1674.

Kinny, P.D., Friend, C.R.L., 1997. U–Pb isotopic evidence for the accretion of different crustal blocks to form the Lewisian Complex of northwest Scotland. Contributions in Mineralogy and Petrology 129, 326–340.

Kinny, P.D., Friend, C.R.L., Love, G.J., 2005. Proposal for a terrane-based nomenclature for the Lewisian gneiss complex of NW Scotland. Journal of the Geological Society, London 162 (1), 175–186.

Mariani, E., Prior, D.J., McNamara, D., Pearce, M.A., Seaton, N., Seward, G.G.E., Tatham, D.J., Wheeler, J., 2009. Electron back-scattered diffraction (EBSD) in the SEM: applications to microstructures in minerals and rocks and recent technological advancements. In: Subias, I., Bauluz, B. (Eds.), Instrumental Techniques Applied to Mineralogy and Geochemistry. Seminarios SEM, 5, pp. 7–19.

Marshall, D.B., McLaren, A.C., 1977a. Deformation mechanisms in experimentally deformed plagioclase feldspars. Physics and Chemistry of Minerals 1 (4), 351–370.

Marshall, D.B., McLaren, A.C., 1977b. Direct observation and analysis of dislocations in experimentally deformed plagioclase feldspars. Journal of Materials Science 12 (5), 893–903.

McLaren, S., Reddy, S.M., 2009. Electron backscatter diffraction analysis of K-feldspar and the relationship between microstructure and 40Ar/39Ar ages. Journal of Structural Geology.

Mehl, L., Hirth, G., 2008. Plagioclase preferred orientation in layered mylonites: evaluation of flow laws for the lower crust. Journal of Geophysical Research 113.

Nyman, M.W., Law, R.D., Smelik, E.A., 1992. Cataclastic deformation mechanism for the development of core-mantle structures in amphibole. Geology 20 (5), 455–458.

Park, R.G., Tarney, J., 1987. The Lewisian complex; a typical Precambrian high-grade terrain?. In: Evolution of the Lewisian and Comparable Precambrian High Grade Terrains Geological Society, London, Special Publications, vol. 27, pp. 13–25.

Pearce, M.A., 2009. Microstructural contraints on the tectonothermal evolution of the Lewisian Gneiss, NW Scotland. Unpublished PhD thesis, University of Liverpool.

Pearce, M.A., Wheeler, J., 2010. Modelling grain-recycling zoning during metamorphism. Journal of Metamorphic Geology 28 (4), 423–437.

Poirier, J.-P., 1985. Creep of Crystals. Cambridge University Press, Cambridge.

Post, A., Tullis, J., 1999. A recrystallized grain size piezometer for experimentally deformed feldspar aggregates. Tectonophysics 303 (1–4), 159–173.

Prior, D.J., Boyle, A.P., Brenker, F., Cheadle, M.C., Day, A., Lopez, G., Peruzzo, L., Potts, G.J., Reddy, S., Spiess, R., Timms, N.E., Trimby, P., Wheeler, J., Zetterstrom, L., 1999. The application of electron backscatter diffraction and orientation contrast imaging in the SEM to textural problems in rocks. American Mineralogist 84 (11–12), 1741–1759.

Prior, D.J., Mariani, E., Wheeler, J., 2009. EBSD in the Earth Sciences: applications, common practice and challenges. In: Schwatz, A.J., Kumar, M., B.L., A., Field, D.P. (Eds.), Electron Backscatter Diffraction in Materials Science. Springer, New York.

Rutter, E.H., Brodie, K.H., 1988. The role of tectonic grain-size reduction in the rheological stratification of the lithosphere. Geologische Rundschau 77 (1), 295–307.

Rybacki, E., Dresen, G., 2000. Dislocation and diffusion creep of synthetic anorthite aggregates. Journal of Geophysical Research-Solid Earth 105 (B11), 26017–26036.

Rybacki, E., Dresen, G., 2004. Deformation mechanism maps for feldspar rocks. Tectonophysics 382 (3–4), 173.

Stünitz, H., 1998. Syndeformational recrystallization – dynamic or compositionally induced? Contributions to Mineralogy and Petrology 131 (2–3), 219–236.

Stünitz, H., Fitz Gerald, J.D., Tullis, J., 2003. Dislocation generation, slip systems, and dynamic recrystallization in experimentally deformed plagioclase single crystals. Tectonophysics 372 (3–4), 215–233.

Sutton, J., Watson, J., 1950. The pre-Torridonian metamorphic history of the Loch Torridon and Scourie areas in the north-west Highlands, and its bearing on the chronological classification of the Lewisian. Quarterly Journal of the Geological Society of London 106 (423), 241–307. Part 3.

Tatham, D.J., Lloyd, G.E., Butler, R.W.H., Casey, M., 2008. Amphibole and lower crustal seismic properties. Earth and Planetary Science Letters 267 (1–2), 118–128.

Vollmer, F.W., 1990. An application of eigenvalue methods to structural domain analysis. Bulletin of the Geological Society of America 102, 786–791.

Wayte, G.J., Worden, R.H., Rubie, D.C., Droop, G.T.R., 1989. A TEM study of disequilibrium plagioclase breakdown at high-pressure – the role of infiltrating fluid. Contributions to Mineralogy and Petrology 101 (4), 426–437.

Wheeler, J., 1987. The determination of true shear senses from the deflection of passive markers in shear zones. Journal of the Geological Society of London 144 (1), 73–77.

Wheeler, J., Windley, B.F., Davies, F.B., 1987. Internal evolution of the major Precambrian shear belt at Torridon, NW Scotland. In: Park, R.G., Tarney, J. (Eds.), Evolution of the Lewisian and Comparable Precambrian High Grade Terrains. Geological Society, London, Special Publications, vol. 27, pp. 153–163.

Wheeler, J., 2007. A major high strain zone in the Lewisian Complex in the Loch Torridon area. In: Ries, A.C., Butler, R.W.H., Graham, R.H. (Eds.), Deformation of

the Continental Crust: The Legacy of Mike Coward. Geological Society, London, Special Publication, vol. 272, pp. 27–45.
Wheeler, J., 2009. The preservation of seismic anisotropy in the Earth's mantle during diffusion creep. Geophysical Journal International 178, 1723–1732.
Wheeler, J., Mariani, E., Piazolo, S., Prior, D.J., Trimby, P., Drury, M.R., 2009. The weighted Burgers vector: a new quantity for constraining dislocation densities and types using electron backscatter diffraction on 2D sections through crystalline materials. Journal of Microscopy-Oxford 233 (3), 482–494.
Wilks, K.R., Carter, N.L., 1990. Rheology of some continental lower crustal rocks. Tectonophysics 182, 57–77.
Wintsch, R.P., Yi, K., 2002. Dissolution and replacement creep: a significant deformation mechanism in mid-crustal rocks. Journal of Structural Geology 24 (6–7), 1179.